Emerging correlations between diffusing particles evolving via simultaneous resetting with memory

Denis Boyer¹ and Satya N. Majumdar²

¹¹Instituto de Física, Universidad Nacional Autónoma de México, Ciudad de México 04510, México ²LPTMS, CNRS, Univ. Paris-Sud, Université Paris-Saclay, 91405 Orsay, France

We study the emergence of correlations between N components of the position of a diffusive walker in N dimensions that starts at the origin and resets to previously visited sites with certain probabilities. This is equivalent to N independent one-dimensional diffusive processes starting from the origin and being subject to simultaneous resetting to positions visited in the past. Resetting follows a memory kernel that interpolates between resetting to the origin only, and the preferential relocation model, a path-dependent process which is highly non-Markov. For weak memory, the correlation coefficient between two components of the N-dimensional process grows monotonously with time and tends at late times to a constant bounded by 1/5, the value corresponding to the non-equilibrium steady state of resetting to the origin. When memory is sufficiently long-ranged, the correlation is non-monotonous and reaches a maximum at a finite time before converging to its asymptotic value. These two regimes are separated by a critical memory parameter value. In the limiting case of the preferential relocation model, the components become uncorrelated at both short and long times, but the correlation vanishes logarithmically slowly at late times. The emergence of correlations through resetting can be described in a unified way in all cases by noticing that the processes are conditionally independent and identically distributed, even in the presence of memory. In the non-Markovian case, the conditioning parameter is the duration of a Brownian path composed of several parts of the full trajectory of a fixed duration t.

I. INTRODUCTION

Resetting is able to substantially alter the dynamics of stochastic processes through the emergence of non-equilibrium steady states (NESSs) and anomalous relaxation [1–3]. In the well-studied example of simple diffusion, the probability density function (PDF) of the position of a Brownian walker, that is interrupted with constant rate and instantaneously restarted from the initial position, tends at late times to a stationary distribution with a broken detailed balance and exhibiting exponential tails. Over the past decade, the characterization of NESSs in diffusive systems subject to resetting has been extended to a variety of resetting protocols [4–9]. Going beyond theoretical studies, diffusion with stochastic resetting has also been realized experimentally in colloidal systems confined by optical traps [10–12].

While the one-dimensional geometry has attracted much attention due to its relative simplicity, a body of research has also focused on the effects of resetting on diffusive processes in higher dimensions [1, 10, 12, 13], or more generally on interacting systems with many degrees of freedom – this includes fluctuating interfaces [14], two interacting Brownian particles [15], symmetric exclusion processes [16], the Ising model evolving under Glauber dynamics [17], the Kuramoto model under subsystem resetting [18], or ballistically moving particles subject to threshold resetting [19] (see [9] and [20] for reviews). Only recently a quite remarkable feature of resetting in dimension larger than one has been unveiled [21]. Consider a single Brownian particle in N dimensions with coordinates $\vec{x}(t) = \{x_1(t), x_2(t), \dots, x_N(t)\}$ that is stochastically reset to the origin with rate r. This problem is equivalent to N independent one-dimensional Brownian motions that are simultaneously reset with rate r to their original values. Even though during the evolution between two consecutive resetting events the processes $\{x_i(t)\}_{i=1,\dots,N}$ evolve independently of each other, the simultaneous resetting introduces strong attractive and all-to-all correlations between them. There correlations grow with time before eventually reaching a non-zero value in the stationary state [21]. This phenomenon of "dynamically induced correlation via simultaneous resetting" between independent particles has subsequently been found in a number of other classical models such as Lévy flights and run-and-tumble particles undergoing simultaneous resetting [22], independent Ornstein-Uhlenbeck particles with a stochastically switching stiffness [23] or a stochastically switching trap centre [24], independent Brownian particles subject to a common diffusing diffusivity [25], or Brownian particles subject to simultaneous resetting but with a non-Poissonian resetting protocol [26]. This mechanism for the emergence of strong correlations has recently been demonstrated experimentally in a system of N colloidal particles in a harmonic optical trap whose stiffness switches stochastically between two values [27]. Finally, similar emergent correlations between independent degrees of freedom induced by simultaneous resetting has also been found in quantum resetting models subject to quantum resetting to the initial state after a random exponentially distributed time. Examples include non-interacting spin chains in a transverse magnetic field [28, 29], and noninteracting bosonic oscillators evolving unitarily after a sudden quench of either the center of the trap [30] or the stiffness of the trap [31].

Processes under simultaneous resetting belong to a wider class of problems with a non-factorizable joint distribution in the stationary state, where the random variables are conditionally independent and identically distributed (c.i.i.d.). In the context of resetting to a fixed position in space (e.g. to the initial position), conditioned on the time interval since the last resetting event, the N variables are actually independent. However, taking the average over this time elapsed since the last resetting event generates attractive all-to-all correlations between pairs. The c.i.i.d. structure is advantageous, as it allows the exact calculation of many physical observables which are usually not easy to compute in strongly correlated systems, such as the average density of particles, the distribution of the extremes, the consecutive spacings between particles, or the full counting statistics [21, 22].

Most of these recent studies on dynamically emergent correlations have considered memory-less stochastic resetting, which occurs to a fixed position or state, and does not depend on the history of the process. The aim of the present study is to investigate the emergence of correlations in a non-Markovian system where resetting occurs more generally to positions visited in the past. Consider for instance an animal in two dimensions with coordinates $\{x_1(t), x_2(t)\}$ that diffuses freely in its environment and revisits from time to time familiar places, i.e., positions visited at previous times. A modelling framework for this type of systems is the preferential relocation model or 'monkey walk', where any past position can be revisited via resetting, with a probability proportional to the total amount of time spent at that position by the walker since the initial time [32–34]. Contrary to the case of resetting to the origin only, this process does not exhibit a NESS at late times but a very slow, logarithmic diffusion. The model also reproduces quantitatively several movement statistics of non-human primates observed in the wild [32]. While these memory processes have been studied theoretically mostly in one dimension, the existence of correlations induced dynamically between the two coordinates $x_1(t)$ and $x_2(t)$ is of possible interest in Ecology and animal foraging. The use of memory by animals in movement has been documented in many species and can be characterised, for instance, from the analysis of long-term trajectories obtained from tracking devices equipping individuals reintroduced in a new environment [35–41]. The study of correlations thus represents a possible way of identifying the use of memory and preferential relocation processes. The goal of this paper is to compute exactly how the correlations between different components evolve with time in the 'monkey walk' model in N dimensions. One of the main results is a striking non-monotonic behaviour of these mutual correlations. The correlations between different components initially grow with time and then eventually decreases to zero very slowly at large times. This feature is very different from the dynamics of mutual correlations in systems with resetting to a single position, where the correlations grow with time monotonically and eventually saturates to a constant value [26].

The rest of the article is organized as follows. In Section II, we introduce a correlation coefficient that quantifies mutual correlations between two processes and show how it can be obtained from the small k expansion of the Fourier transform of their joint PDF. In Section III we apply this method to compute the mutual correlations in a resetting model with memory in N dimensions, that is characterized by an exponential memory kernel with parameter λ . Section III A presents results on the limiting case of resetting to the origin $(\lambda \to \infty)$, while Section III B is devoted to the analysis of the opposite limit $\lambda \to 0$ corresponding to the preferential relocation model. In Section IV, we compute the correlations in the general case at λ finite, first in the infinite time limit (IV A) and then at finite times (IV B). In Section V, we show that models with resetting and memory generally admit a hidden c.i.i.d. structure, that extends the standard renewal approach of memory-less resetting processes and allows us to describe the emergence of correlations in a unified way in these systems. Conclusions are presented in Section VI and technical details in Appendix A.

II. QUANTIFYING CORRELATIONS BETWEEN TWO PROCESSES

Let us consider a process $\vec{x}(t)$ in N dimensions with components $\{x_i(t)\}_{i=1,...,N}$ that have the same initial condition $x_i(t=0) = 0$ and the same marginal PDF $p(x_i,t)$. We focus on the correlations between two components, say $x_1(t)$ and $x_2(t)$. The natural measure of correlations among two variables is the 2×2 matrix defined by

$$C_{ij}(t) = \langle x_i(t)x_j(t)\rangle - \langle x_i(t)\rangle\langle x_j(t)\rangle, \quad i = \{1, 2\}, \ j = \{1, 2\}.$$

$$(1)$$

We first notice that if the joint PDF $P(\vec{x},t)$ is invariant under permutation of the labels of the axis or particles, for instance due to isotropy, the correlation $C_{ii}(t)$ is the same for all i, while $C_{ij}(t)$ is also the same for any pair of indices (i,j) with $i \neq j$. Secondly, the diffusive problems considered in the next Sections are also symmetrical under an inversion $x \to -x$, hence the mean $\langle x_i(t) \rangle = 0$ at all times t for any t. In addition, the function $C_{ij}(t)$ with $i \neq j$ is also identically zero by symmetry at all times t, as the points (x_1, x_2) and $(-x_1, x_2)$ turn out to have the same probability density. Hence, to detect a non-zero correlation between $x_1(t)$ and $x_2(t)$, it is necessary to focus on another 2×2 correlation matrix, such as

$$A_{ij}(t) = \langle x_i^2(t) x_j^2(t) \rangle - \langle x_i^2(t) \rangle \langle x_j^2(t) \rangle, \quad i = \{1, 2\}, \ j = \{1, 2\}.$$
 (2)

Let us call $\lambda_{+}(t)$ and $\lambda_{-}(t) \leq \lambda_{+}(t)$ the eigenvalues of **A**, and define the time-dependent correlation coefficient of the two processes as

$$a(t) \equiv \frac{\lambda_{+}(t) - \lambda_{-}(t)}{\lambda_{+}(t) + \lambda_{-}(t)}.$$
 (3)

Since $x_1(t)$ and $x_2(t)$ are identically distributed, $A_{11}(t) = A_{22}(t) = \langle x_1^4(t) \rangle - \langle x_1^2(t) \rangle^2$ and $A_{12}(t) = A_{21}(t) = \langle x_1^2(t) x_2^2(t) \rangle - \langle x_1^2(t) \rangle^2$. After straightforward algebra, the parameter a(t) reads

$$a(t) = \frac{\langle x_1^2(t)x_2^2(t)\rangle - \langle x_1^2(t)\rangle^2}{\langle x_1^4(t)\rangle - \langle x_1^2(t)\rangle^2}.$$
 (4)

This quantity lies in the interval [0, 1], with the limiting cases a(t) = 0 if the processes are independent at all times, while a(t) = 1 for perfectly correlated processes, i.e., $x_2(t) = x_1(t)$ or $x_2(t) = -x_1(t)$.

In the examples to be analysed below, the Fourier transform of the joint distribution,

$$\tilde{P}(\vec{k},t) = \int d\vec{x} \, e^{i\vec{k}\cdot\vec{x}} P(\vec{x},t) \,, \tag{5}$$

only depends on the components $\{k_i\}$ of \vec{k} through its square modulus $k^2 = k_1^2 + k_2^2 + \ldots + k_N^2$ at all times t. Let us suppose that $\tilde{P}(\vec{k},t)$ can be expanded in power series at small k^2 ,

$$\tilde{P}(\vec{k},t) = 1 - c_2(t) k^2 + c_4(t) k^4 + \dots,$$
(6)

where the term of order k^0 comes from the normalization of $P(\vec{x}, t)$. Clearly, $C_{12}(t)$ in Eq. (1) vanishes identically at all times t. This follows from the fact that

$$\langle x_1(t)x_2(t)\rangle = -\left. \frac{\partial^2 \tilde{P}(\vec{k},t)}{\partial k_1 \partial k_2} \right|_{\vec{k}=\vec{0}} = 0,$$
 (7)

where the last equality is a consequence of Eq. (6). We similarly deduce the general relations,

$$\langle x_1^2(t)\rangle = -\left. \frac{\partial^2 \tilde{P}(\vec{k}, t)}{\partial k_1^2} \right|_{\vec{k} = \vec{0}} = 2 c_2(t), \qquad (8)$$

$$\langle x_1^4(t) \rangle = \frac{\partial^4 \tilde{P}(\vec{k}, t)}{\partial k_1^4} \bigg|_{\vec{k} = \vec{0}} = 24 c_4(t) ,$$
 (9)

$$\langle x_1^2(t)x_2^2(t)\rangle = \frac{\partial^4 \tilde{P}(\vec{k},t)}{\partial k_1^2 \partial k_2^2} \bigg|_{\vec{k}=\vec{0}} = 8 c_4(t) ,$$
 (10)

and obtain from Eq. (4),

$$a(t) = \frac{2c_4(t) - c_2^2(t)}{6c_4(t) - c_2^2(t)}. (11)$$

Hence the knowledge of $c_2(t)$ and $c_4(t)$ yields the correlation coefficient a(t), which is the main quantity of interest here. Note that due to the isotropic structure of Eq. (6) and the subsequent relations (9)-(10), one has $\langle x_1^2(t)x_2^2(t)\rangle = \frac{1}{3}\langle x_1^4(t)\rangle < \langle x_1^4(t)\rangle$. Therefore the variables x_1 and x_2 cannot be perfectly correlated and a(t) < 1.

III. DIFFUSION WITH SIMULTANEOUS RESETTING AND A MEMORY KERNEL $\phi(\tau) = e^{-\lambda \tau}$

We consider a particle diffusing in N spatial dimensions and starting at the origin [or, equivalently, N independent particles diffusing on a line with initial positions $x_i(t=0)=0$, with $i=1,\ldots,N$]. With rate r, the particle resets to a previously visited position according to the following protocol. The particle keeps track of its own trajectory $\vec{x}(\tau)$ for $0 \le \tau \le t$. In a small time interval $[t,t+\Delta t]$, with probability $r\Delta t$ the particle chooses a previous time instant τ distributed with a PDF $K_t(\tau)$ and resets to the position occupied at that time τ , i.e., $\vec{x}(t+\Delta t) = \vec{x}(\tau)$. Hence, considering each component of \vec{x} as a particle in 1d, the resetting event occurs simultaneously for all the N particles and they choose the same time τ in the past. A discrete-time version of this model of resetting with memory for N=1 particle was introduced and studied in Ref. [32]. The generalisation to continuous-time was studied in Ref. [33]. Here we further generalise this continuous-time model to N>1. Our goal is to study how dynamical correlations between the coordinates of \vec{x} emerge when resetting involves memory, i.e., a function $K_t(\tau)$ which is not simply $\delta(\tau)$ that characterises the kernel associated with memory-less resetting to the origin.

Let $P_r(\vec{x},t)$ denote the joint PDF of the components of \vec{x} at time t under resetting with memory. This quantity evolves via the Fokker-Planck equation

$$\partial_t P_r(\vec{x}, t) = D \nabla^2 P_r(\vec{x}, t) - r P_r(\vec{x}, t) + r \int_0^t d\tau \int_{-\infty}^\infty d\vec{x}' K_t(\tau) P_r^{(2)}(\vec{x}', t; \vec{x}, \tau), \qquad (12)$$

starting from the initial condition $P_r(\vec{x},t=0) = \delta(\vec{x})$. The first term on the right-hand-side (rhs) just represents diffusion and D is the diffusion constant. The second term represents the loss from position \vec{x} due to simultaneous resetting with resetting rate r. The third term represents the gain term to position \vec{x} via resetting from a position \vec{x}' reached at time t, where $P_r^{(2)}(\vec{x}',t;\vec{x},\tau)$ represents the joint probability density that the system was at \vec{x} at time $\tau \leq t$ and at \vec{x}' at time t. We need to integrate over all the times τ that can be chosen by the particle, and over all the positions \vec{x}' from which the particle may arrive at \vec{x} by resetting. The reason for the solvability for the one-time marginal position distribution $P_r(\vec{x},t)$ in this model can then be traced back to the fact that

$$\int P_r^{(2)}(\vec{x}', t; \vec{x}, \tau) d\vec{x}' = P_r(\vec{x}, \tau), \qquad (13)$$

leading to a closed equation for the one-time PDF

$$\partial_t P_r(\vec{x}, t) = D \nabla^2 P_r(\vec{x}, t) - r P_r(\vec{x}, t) + r \int_0^t d\tau K_t(\tau) P_r(\vec{x}, \tau).$$

$$\tag{14}$$

We next assume that $K_t(\tau)$ takes the form,

$$K_t(\tau) = \frac{\phi(\tau)}{\int_0^t dt' \,\phi(t')},\tag{15}$$

with $\phi(\tau)$ a non-negative function, and where the denominator in Eq. (15) ensures normalization, i.e., $\int_0^t d\tau K_t(\tau) = 1$. In the following, we will consider an exponential kernel,

$$\phi(\tau) = e^{-\lambda \tau},\tag{16}$$

with λ a non-negative constant. Hence the walker tends to privilege the positions occupied at early times for resetting. This model interpolates between two well-studied cases.

When $\lambda \to \infty$, the particle resets to the initial position only. In this case $K_t(\tau) = \delta(\tau)$ and Eq. (14) becomes

$$\partial_t P_r(\vec{x}, t) = D \nabla^2 P_r(\vec{x}, t) - r P_r(\vec{x}, t) + r \delta(\vec{x}). \tag{17}$$

At late times, $P_r(\vec{x},t)$ approaches a NESS, $P^*(\vec{x})$, whose expression in N dimension is given in Refs. [1, 13].

When $\lambda \to 0$, the random variable τ is distributed uniformly in the interval [0,t], or $K_t(\tau) = 1/t$. This case corresponds to the preferential relocation model [32, 33] (or monkey walk [34]), where the probability density for choosing a position \vec{x} for revisit is proportional to the local time spent by the walker at that site since the beginning of the process. Hence, more frequently visited regions of space are more likely to be revisited again. The Fokker-Planck equation (14) becomes

$$\partial_t P_r(\vec{x}, t) = D \nabla^2 P_r(\vec{x}, t) - r P_r(\vec{x}, t) + \frac{r}{t} \int_0^t d\tau \ P_r(\vec{x}, \tau) \,. \tag{18}$$

This process has long range memory and is therefore highly non-Markov. At late times, as recalled further in Section IIIB, the joint PDF above does not approach a NESS and remains time-dependent. The variance $\langle \vec{x}^2 \rangle(t)$ keeps growing unbounded although very slowly, as it is proportional to $\ln(rt)$.

Our goal is to compute the correlation coefficient $a_{\lambda}(t)$ given by Eq. (11) which now depends on λ , t and r (which is kept implicit in the notation). In the next sub-sections, we show that $a_{\lambda}(t)$ can be obtained exactly at all times in these two limiting cases, namely $\lambda \to \infty$ and $\lambda \to 0$.

A. Resetting to the origin, i.e., the limit $\lambda \to \infty$

In the limit $\lambda \to \infty$, one obtains $K_t(\tau) = \delta(\tau)$ and this case simply corresponds to the memory-less simultaneous resetting of all the components to the origin. In this limiting case, the matrix elements $A_{ij}(t)$ in Eq. (2) were computed exactly for all t in Ref. [26]. We reproduce below this calculation for the sake of completeness and compute the correlation coefficient $a_{\lambda \to \infty}(t) \equiv a_{\infty}(t)$ explicitly.

Instead of solving Eq. (17), it is more convenient to write directly the solution $P_r(\vec{x},t)$ in the form of a renewal process [9],

$$P_r(\vec{x},t) = e^{-rt}G_0(\vec{x},t) + r \int_0^t dt' \, e^{-rt'}G_0(\vec{x},t'), \tag{19}$$

with $G_0(\vec{x},t)$ the propagator of free diffusion in N dimensions,

$$G_0(\vec{x},t) = \frac{1}{(4\pi Dt)^{\frac{N}{2}}} \exp\left(-\frac{\vec{x}^2}{4Dt}\right) = \prod_{i=1}^{N} \frac{1}{\sqrt{4\pi Dt}} e^{-\frac{x_i^2}{4Dt}}.$$
 (20)

The first term in the rhs of Eq. (19) counts the trajectories that reached \vec{x} by diffusing freely because they never reset up to time t. The second term accounts for the trajectories that last restarted from the origin at a time t - t' > 0 and then diffused freely from there until time t without further resetting. Taking the Fourier transform of Eq. (19), one obtains

$$\tilde{P}_r(\vec{k},t) = e^{-(r+Dk^2)t} + r\frac{1 - e^{-(r+Dk^2)t}}{r + Dk^2},$$
(21)

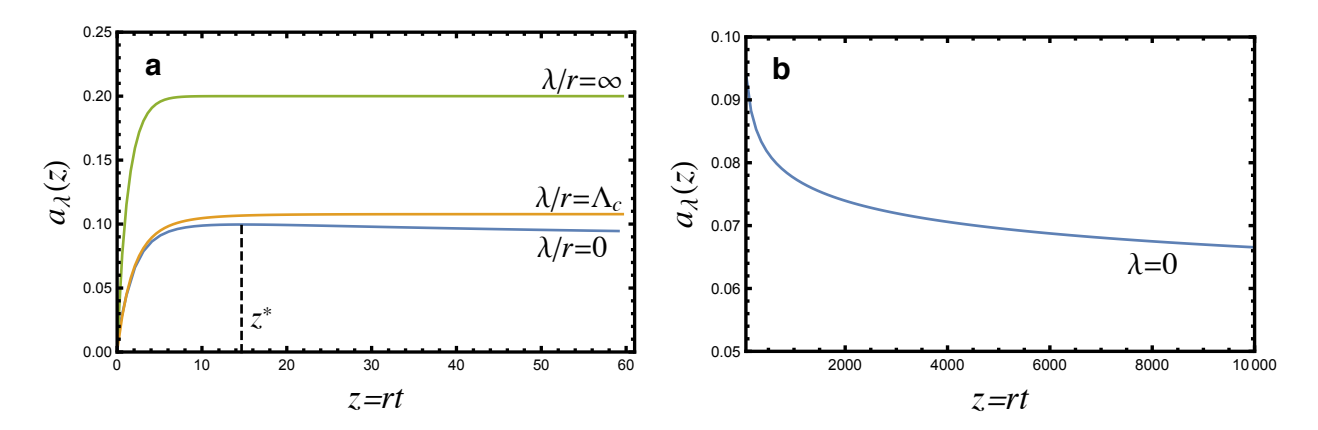


FIG. 1. (a) Correlation coefficient $a_{\lambda}(z)$ defined in Eq. (11) as a function of the rescaled time z=rt, for various particular values of λ . The case $\lambda=\infty$ (resetting to the origin) is given by Eq. (25) and tends exponentially fast to the asymptotic value 1/5. In the case $\lambda=0$ (preferential relocation model), $a_0(z)$ is obtained from Eqs. (41)-(42) and exhibits a non-monotonous behaviour with a maximum at $z^*=14.6732...$ The correlation $a_0(z)$ increases linearly at small z and, as shown by Panel (b) on a different scale of values of z, decays very slowly to 0 at large z, as $1/\ln z$ to leading order. For all $\lambda>0$, $a_{\lambda}(z)$ tends to finite value as $z\to\infty$, which depends on λ/r only and is given by Eqs. (53)-(54). For $\lambda/r<\Lambda_c=0.0743...$, $a_{\lambda}(z)$ has a maximum at a finite $z^*(\lambda/r)$, whereas for $\lambda/r \geq \Lambda_c$, $a_{\lambda}(z)$ increases monotonously with z like in the case $\lambda=\infty$.

The expansion of the above expression up to order k^4 gives, in the notation of Eq. (6),

$$c_2(z) = \frac{D}{r} \left(1 - e^{-z} \right) \tag{22}$$

$$c_4(z) = \frac{D^2}{r^2} \left[1 - (1+z) e^{-z} \right] , \qquad (23)$$

where we have defined the rescaled time variable,

$$z \equiv rt. \tag{24}$$

Therefore the correlation coefficient $a_{\infty}(t)$ defined in Eq. (4) is obtained from Eq. (11) and only depends on z,

$$a_{\infty}(z) = \frac{1 - 2ze^{-z} - e^{-2z}}{5 - (4 + 6z)e^{-z} - e^{-2z}}.$$
 (25)

We deduce $a_{\infty}(z \to \infty) = 1/5 > 0$, hence the correlation between the components (or particles) $x_1(t)$ and $x_2(t)$ persists in the steady state. The asymptotic behaviours are given by,

$$a_{\infty}(z) = \frac{1}{5} - \frac{4}{25}ze^{-z} + \mathcal{O}(e^{-z}) \quad \text{as} \quad z \to \infty,$$
 (26)

and

$$a_{\infty}(z) = \frac{z}{6} - \frac{z^2}{12} + \mathcal{O}(z^3)$$
 as $z \to 0$. (27)

The variations of $a_{\infty}(z)$ with z are displayed in Fig. 1a (top curve). The correlation coefficient is monotonously increasing, illustrating the building of dynamical correlations over time through resetting to the origin.

B. Resetting with preferential relocation, or limit $\lambda \to 0$

In this case, we start from the Fourier transform of Eq. (18),

$$\partial_t \tilde{P}_r(\vec{k}, t) = -(r + Dk^2) \tilde{P}_r(\vec{k}, t) + \frac{r}{t} \int_0^t \tilde{P}_r(\vec{k}, \tau) d\tau$$
(28)

where we recall that $k^2 = k_1^2 + k_2^2 + \ldots + k_N^2$. In fact, Eq. (28) is a straightforward generalization of the N = 1 case (only k_1^2 gets replaced by k^2). Using the exact solution for N = 1 given in Ref. [33] and replacing k_1^2 by k^2 provides the exact solution for the N-particle case,

$$\tilde{P}_r(\vec{k},t) = M\left(\frac{Dk^2}{r + Dk^2}, 1, -(r + Dk^2)t\right),$$
(29)

where M(b, c, u) is the Kummer's confluent hypergeometric function defined by the power series

$$M(b,d,u) = \sum_{n=0}^{\infty} \frac{(b)_n u^n}{(d)_n n!}.$$
 (30)

Here $(b)_n = b(b+1)(b+2)\dots(b+n-1)$ is the Pochhammer symbol for $n \ge 1$, with $(b)_0 = 1$.

The exact solution (29) clearly demonstrates that at any finite time t, the particle positions are correlated, too, because $\tilde{P}(\vec{k},t)$ does not factorise into a product of indepedent marginal distributions. Consequently, in real space, the joint distribution does not factorise,

$$P_r(\vec{x}, t) \neq p_r(x_1, t)p_r(x_2, t)\dots p_r(x_N, t),$$
 (31)

where $p_r(x_1,t) = \int P_r(x_1,x_2,\ldots,x_N,t)dx_2\,dx_3\ldots dx_N$ is the marginal distribution of the first particle and so on. Clearly, this correlation is induced dynamically via simultaneous resetting in the presence of memory.

Before calculating the correlation coefficient $a_{\lambda=0}(t) \equiv a_0(t)$ for all times, let us first investigate the limit of very large times $t \to \infty$. In this case, using the asymptotic behaviour [42],

$$M(b,d,u) \approx \frac{\Gamma(d)}{\Gamma(d-b)} (-u)^{-b} \quad \text{as} \quad u \to -\infty,$$
 (32)

in Eq. (29), we get, to leading order for large t,

$$\tilde{P}_r(\vec{k}, t) \approx \frac{1}{\Gamma\left(\frac{r}{r + Dk^2}\right)} e^{-\frac{Dk^2}{r + Dk^2} \ln[(r + Dk^2)t]}.$$
(33)

Furthermore, taking the small k and large t limits, keeping $k^2 \ln(rt)$ fixed, we get the asymptotic (long-distance long-time) scaling behaviour

$$\tilde{P}_r(\vec{k}, t) \approx e^{-\frac{D}{r}\ln(rt)k^2} = \prod_{i=1}^N e^{-\frac{D}{r}\ln(rt)k_i^2}$$
 (34)

Thus, in this scaling limit, the Fourier transform of the joint PDF does indeed factorise. By inverting the Fourier transform, the joint PDF in the real space just becomes a product of Gaussians,

$$P(\vec{x}, t) \approx \prod_{i=1}^{N} \frac{1}{\sqrt{2\pi\sigma^2(t)}} e^{-x_i^2/2\sigma^2(t)} \quad \text{where} \quad \sigma^2(t) = \frac{2D}{r} \ln(rt).$$
 (35)

Therefore, in the long time scaling limit, the variables $x_i(t)$ become statistically independent of each other, implying $a_0(t) \to 0$ as $t \to \infty$. In addition, the distribution of each variable converges to a Gaussian with zero mean and variance $\sigma^2(t)$ growing logarithmically with time. Note that the variance of $\vec{x}(t)$ is obtained by summing over the N components, or $\langle \vec{x}^2(t) \rangle \simeq \frac{2DN}{r} \ln(rt)$. Clearly, there is no correlation between the components of $\vec{x}(t)$ at short times neither, as they are essentially independent Brownian motions. So, the correlation $a_0(t)$ must behave non-monotonically with t.

To extract the coefficients $c_2(t)$ and $c_4(t)$ of the small k expansion (6) at any time, it is useful to expand Eq. (29) in power series using Eq. (30). This gives, after small rearrangements,

$$\tilde{P}_r(\vec{k},t) = 1 + Dk^2 \sum_{n=1}^{\infty} (2Dk^2 + r)(3Dk^2 + 2r) \dots (nDk^2 + r(n-1)) \frac{(-t)^n}{(n!)^2}.$$
(36)

Expanding up to order $\mathcal{O}(k^4)$ is simple to do. Indeed, it is easy to see that for $n \geq 2$,

$$(2Dk^{2} + r)(3Dk^{2} + 2r)\dots(nDk^{2} + r(n-1)) = (n-1)!\left[r^{n-1} + r^{n-2}(n-1 + H_{n-1})Dk^{2} + O(k^{4})\right],$$
(37)

where $H_n = 1 + 1/2 + 1/3 + \ldots + 1/n$ is the harmonic number. For n = 1 in Eq. (36), the coefficient of -t is simply Dk^2 . Putting this result back into (36) gives

$$\tilde{P}_r(\vec{k}, t) = 1 + \frac{Dk^2}{r} \sum_{n=1}^{\infty} \left[1 + (n - 1 + H_{n-1}) \frac{Dk^2}{r} + \mathcal{O}(k^4) \right] \frac{(-rt)^n}{n \, n!} \,, \tag{38}$$

where we interpret $H_0 = 0$. Using the rescaled time z = rt, we deduce

$$c_2(z) = -\frac{D}{r} \sum_{n=1}^{\infty} \frac{(-z)^n}{n \, n!} \,, \tag{39}$$

and

$$c_4(z) = \frac{D^2}{r^2} \sum_{n=2}^{\infty} (n - 1 + H_{n-1}) \frac{(-z)^n}{n \, n!} \,. \tag{40}$$

The two above sums can be carried out by using Mathematica and can be rewritten as,

$$c_2(z) = \frac{D}{r} \left[E_1(z) + \gamma_E + \ln z \right] , \tag{41}$$

and

$$c_4(z) = \frac{D^2}{r^2} \left[\gamma_E - 1 + E_1(z) + \ln z + e^{-z} + \frac{1}{2} {}_1 F_1^{(2,0,0)}(0,1,-z) \right], \tag{42}$$

where $\gamma_E = 0.5772...$ is the Euler constant, $E_1(z) = \int_z^\infty \frac{e^{-x}}{x} dx$ and ${}_1F_1^{(2,0,0)}(0,1,-z) = \partial_b^2 M(b,1,-z)\Big|_{b=0}$ with M(b,d,u) defined in Eq. (30). Substituting (41) and (42) in the expression (11) gives the sought coefficient $a_0(z)$, which also only depends on z. The function $a_0(z)$ is plotted in Fig. 1a (bottom curve). Numerically, we find that the correlation is maximal at $z=z^*$ with

$$z^* = 14.6732\dots (43)$$

And at the maximum,

$$a_0(z^*) = 0.0995506...,$$
 (44)

indicating a weaker correlation than in the previous case of resetting to the origin. The asymptotic behaviours are,

$$a_0(z) = \begin{cases} \frac{1}{18} z + O\left(z^2\right) & \text{as} \quad z \to 0\\ \frac{1}{\ln z} + O\left(\frac{1}{\ln^2 z}\right) & \text{as} \quad z \to \infty. \end{cases}$$

$$(45)$$

The correlation thus tends extremely slowly to 0 at large z, as illustrated by Fig. 1b on a different scale, meaning that the components remain correlated during a very long time in practice. While the small t behaviour is easy to extract, computing the large t asymptotics is a bit tricky since Mathematica is unable to provide it. However the precise asymptotics for large t, leading to the second line in Eq. (45), is derived in Appendix A.

IV. CORRELATION IN THE GENERAL CASE $0 < \lambda < \infty$

We now consider the exponential memory kernel (16) for any $\lambda > 0$. The Fourier transform of Eq. (14) reads

$$\partial_t \tilde{P}_r(\vec{k}, t) = -(r + Dk^2) \tilde{P}_r(\vec{k}, t) + \frac{\lambda r}{1 - e^{-\lambda t}} \int_0^t e^{-\lambda \tau} \tilde{P}_r(\vec{k}, \tau) d\tau.$$

$$(46)$$

As for the preferential relocation model, Eq. (46) was exactly solved for the N=1 dimensional case in Ref. [33]. We can then use that solution, replacing k_1^2 by k^2 to obtain the solution in N dimensions,

$$\tilde{P}_{r}(\vec{k},t) = \frac{\Gamma(1-C)}{\Gamma(1-A)\Gamma(1-B)} F(A,B,C;e^{-\lambda t})
+ \frac{1}{1-C} \frac{\Gamma(C)}{\Gamma(A)\Gamma(B)} e^{-\lambda(1-C)t} F(1-B,1-A,2-C;e^{-\lambda t}),$$
(47)

where $F(u, v, w; \chi)$ is the standard hypergeometric function,

$$F(u, v, w; \chi) = \sum_{n=0}^{\infty} \frac{(u)_n (v)_n}{(w)_n} \frac{\chi^n}{n!},$$
(48)

and

$$C = 1 - \frac{r + Dk^2}{\lambda} \tag{49}$$

$$A = \frac{1}{2} \left(C + \sqrt{C^2 + \frac{4Dk^2}{\lambda}} \right) \tag{50}$$

$$B = \frac{1}{2} \left(C - \sqrt{C^2 + \frac{4Dk^2}{\lambda}} \right). \tag{51}$$

A. Infinite time limit

We first analyse the correlation $a_{\lambda}(z)$ in the limit $z = rt \to \infty$, which is more tractable than the finite time case. At late times, $\tilde{P}_r(\vec{k},t)$ in Eq. (47) tends to a NESS given by,

$$\tilde{P}_r^{(\text{st})}(\vec{k}) = \frac{\Gamma(1-C)}{\Gamma(1-A)\Gamma(1-B)},$$
(52)

for all $\lambda > 0$ and r > 0. By expanding the expression (52) up to order k^4 and using Eq. (11), one finds that the correlation at infinite time is non-zero, like in the case of resetting to the origin $\lambda = \infty$, and that it is a function of r/λ only,

$$a_{\lambda}(z \to \infty) = f\left(\frac{r}{\lambda}\right)$$
, (53)

with

$$\frac{1}{f(y)} = 3 - \frac{12(y-1)[\gamma_E + \psi(y)]^2}{(y-1)[\pi^2 + 6(2y-1)\psi'(y)] - 12y[\gamma_E + \psi(y)]},$$
(54)

where $\psi(y) = \Gamma'(y)/\Gamma(y)$ is the polygamma function of 0-th order. The function $a_{\lambda}(z \to \infty)$ has the following asymptotic behaviours with respect to the variable λ/r :

$$a_{\lambda}(z \to \infty) = \begin{cases} -\frac{1}{\ln(\lambda/r)} + \dots & \text{as } \lambda/r \to 0 \\ \frac{1}{5} - \frac{4}{25} \left(\frac{\lambda}{r}\right)^{-1} + \dots & \text{as } \lambda/r \to \infty \end{cases}$$
 (55)

Hence the value of the correlation $a_{\lambda}(z \to \infty)$ at large times is a monotonically increasing function of the rescaled memory parameter $\Lambda \equiv \lambda/r$. The asymptotic correlation grows from 0 to 1/5, as shown by Fig. 2. Due to the logarithmic singularity in the first line of Eq. (55), as soon as $\Lambda \sim 10^{-2}$, the asymptotic correlation is quite large already (~ 0.1).

B. Correlation at finite time

This case is the most general here, as the correlation $a_{\lambda}(t)$ depends on the three variables λ , r and t [the diffusion constant D cancels out between the numerator and denominator of Eq. (11)]. Using the Π -theorem of dimensional analysis [43] and noticing that a_{λ} is dimensionless, the correlation must depend on two dimensionless variables, for instance,

$$a_{\lambda}(t) = \alpha(rt, \lambda/r) = \alpha(z, \Lambda),$$
 (56)

with α a function. The above relation actually allows us to check a posteriori that in the limits $\lambda \to 0$ or $\lambda \to \infty$, the correlation only depends on z = rt. Conversely, for a finite λ but $t \to \infty$, it only depends on $\Lambda = \lambda/r$ given explicitly

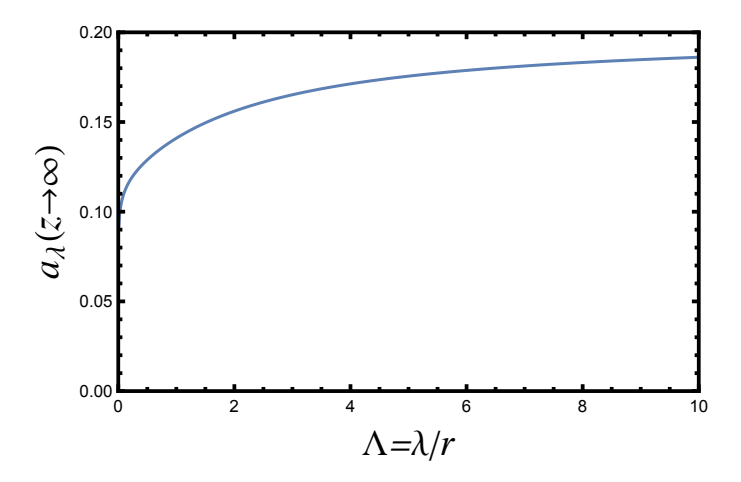


FIG. 2. Asymptotic value of the correlation at large times as a function of $\Lambda = \lambda/r$.

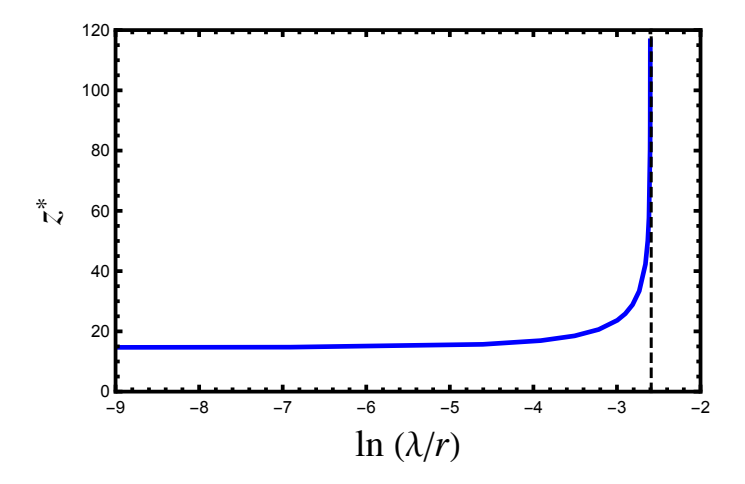


FIG. 3. Rescaled time z^* where the correlation $a_{\lambda}(z)$ is maximal, depicted in Fig. 1, as a function of λ/r (in log scale). For $\lambda/r < \Lambda_c = 0.0743\ldots, z^*$ is finite and $a_{\lambda}(z)$ non-monotonous. For $\lambda/r > \Lambda_c$, or a memory kernel sufficiently peaked at short times, $a_{\lambda}(z)$ increases monotonously with z and the maximal correlation is reached at infinite times $(z^* = \infty)$. The vertical dashed line shows the location of the critical value $\ln(\Lambda_c) = \ln(0.0743\cdots) = -2.59964\ldots$

in Eqs. (53) and (54). Extracting the coefficients $c_2(t)$ and $c_4(t)$ from Eq. (47) at finite t is cumbersome and we have opted to perform the Taylor expansion in powers of k^2 numerically instead. Setting $K \equiv k^2$, the coefficients are obtained from the relations $c_2(t) = -\partial \tilde{P}_r(K,t)/\partial K|_{K=0}$ and $c_4(t) = \frac{1}{2!} \partial^2 \tilde{P}_r(K,t)/\partial K^2|_{K=0}$, where the derivatives of the solution (47) are evaluated numerically with Mathematica.

Figure 1a shows the obtained correlation $a_{\lambda}(z)$ as a function of z, fixing $\Lambda=0.0743\ldots$ (middle curve). We find that this value is peculiar, in the sense that it separates two different regimes. For $0 \le \Lambda < 0.0743\ldots$, the function $\alpha(z,\Lambda)$ is non-monotonous with z and exhibits a maximum at a certain time $z^*(\Lambda)$, like in the case $\lambda=0$. For $\Lambda>0.0743\ldots$, however, $\alpha(z,\Lambda)$ is a monotonous function of z and reaches its maximum at $z=\infty$, like for $\lambda=\infty$. In Fig. 3, we display z^* as a function of Λ . Remarkably, z^* increases with Λ and diverges when $\Lambda \to \Lambda_c = 0.0743\ldots$ from below.

V. RENEWAL-LIKE EQUATION FOR RESETTING WITH MEMORY

In this section we show that the emergence of correlations in processes with simultaneous resetting to the initial position or to sites visited in the past can be described in a unified way by noticing their connection with conditionally independent and identically distributed (c.i.i.d.) random variables [21–26, 30, 31]. Consider first the case $\lambda \to \infty$ where a single Brownian walker in N dimensions resets to the origin with rate r, or equivalently N independent one-dimensional Brownian motions reset simultaneously to the origin with rate r. The renewal equation (19) describes the joint PDF of the N components of the position \vec{x} of the single walker at time t. This renewal equation (19) can

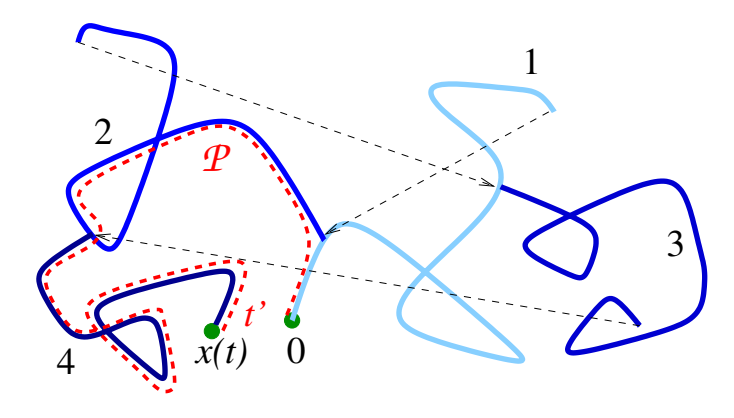


FIG. 4. Illustration of a two-dimensional diffusion process after 3 resetting events to previous positions, or 4 consecutive paths. The long-range jumps to previous points of the trajectory are shown by dashed arrows. The position $\vec{x}(t)$ of the particle at time t can also be reached by following the continuous Brownian path \mathcal{P} (in red), which is of much shorter duration t'. The components of the position $\vec{x}(t)$ have a c.i.i.d. structure.

be expressed in a more convenient form,

$$P_r(\vec{x}, t) = \int_0^\infty dt' \ \varphi_t(t') \prod_{i=1}^N p_0(x_i, t') \,, \tag{57}$$

where $\varphi_t(t') = e^{-rt'}\delta(t'-t) + re^{-rt'}$ for $t' \leq t$ and $\varphi_t(t') = 0$ for t' > t, while $p_0(x_i, t') = G_0(x_i, t') = e^{-x_i^2/4Dt'}/\sqrt{4\pi Dt'}$ is the propagator of a free Brownian motion in 1d. The function $\varphi_t(t')$ represents the PDF of the time t' elapsed between the latest restart and the current time t. Conditioned on t', the variables x_i 's are actually uncorrelated as indicated by the product of the p_0 's, but the presence of the integral over t' correlates them. Consequently, the joint PDF $P_r(\vec{x},t)$ cannot be written as a product of functions of one variable x_i . The structure given by Eq. (57) defines conditionally i.i.d. variables more generally, where t' can be seen as a random parameter with a certain distribution that may or may not depend on t [22].

We now turn to the case of resetting with memory and a general kernel. It turns out that the joint distribution $P_r(\vec{x},t)$ in this case can also be written under an exact form with a structure very similar to Eq. (19), namely,

$$P_r(\vec{x},t) = e^{-rt}G_0(\vec{x},t) + \int_0^\infty dt' \,\Psi_t(t') \,G_0(\vec{x},t') \,, \tag{58}$$

or equivalently

$$P_r(\vec{x}, t) = \int_0^\infty dt' \, \Phi_t(t') \, \prod_{i=1}^N \, p_0(x_i, t') \,, \tag{59}$$

with $\Phi_t(t') = e^{-rt'}\delta(t'-t) + \Psi_t(t')$ and $p_0(x_i,t') = G_0(x_i,t') = e^{-x_i^2/4Dt'}/\sqrt{4\pi Dt'}$ denoting again the one dimensional free Brownian propagator. Eq. (59) has a c.i.i.d. structure like Eq. (57). However, the time t' has a quite different meaning and its PDF $\Phi_t(t')$ is no longer given by $\varphi_t(t')$. The definition of t' is illustrated in Fig. 4 with a twodimensional process (N=2), and can be explained as follows. The first term in the rhs of Eq. (58), represents, as in standard resetting, the probability that the particle has never reset up to time t and has reached the position \vec{x} by pure diffusion. This term is negligible at late times. In the case of one or multiple resetting events, one can notice that the position $\vec{x}(t)$ can be reached from the initial position 0 by following a continuous path \mathcal{P} free of resetting jumps between distant positions (as shown by a red dashed line in Fig. 4). This is a consequence of the fact that resetting occurs to previously visited positions. In Fig. 4, for instance, the particle performs a first Brownian path starting from the origin and resets to a previous position and the path 2 starts from this location. At the end of path 2, the chosen time in the past τ belongs to path 1 and the corresponding position is the beginning of path 3. Similarly, path 4 starts from a point belonging to path 2 and the particle arrives at x(t) without further resetting. On this trajectory, a plain Brownian particle could have reached $\vec{x}(t)$ by taking a piece of path 1 (for a time t_1'), then a piece of path 2 (for a time t_2), and finally all path 4 (of duration t_4). This defines the continuous path \mathcal{P} in red in Fig. 4, while t' is the duration of \mathcal{P} , i.e., $t' = t'_1 + t'_2 + t'_4$ in our example. For any trajectory $\{\vec{x}(t'')\}_{0 \le t'' \le t}$ up to an arbitrary time t, there exists a unique path \mathcal{P} and time $t' \leq t$.

In standard resetting to the origin, the relevant part of the trajectory is the most recent Brownian path starting from the origin following the last reset to the origin. But for resetting with memory, the relevant path is now \mathcal{P} , which also starts from the origin and is Brownian, since it is composed of a succession of independent Brownian motions. The quantity t' now denotes the duration of \mathcal{P} , and not the time since last resetting as in standard resetting to the origin. Having provided a clear physical meaning of the relevant time t', we then note that conditioned on t', the variables x_i 's are distributed with $G_0(\vec{x}, t')$ and independent. These considerations lead to Eq. (59), where the PDF of t' at time t is $\Phi_t(t')$.

Thus, while the c.i.i.d structure of the joint distribution is manifest in Eq. (59), the real non-trivial problem is to determine the distribution $\Phi_t(t')$ of t' for a fixed t. Employing a mapping to weighted random recursive trees, Mailler and Uribe Bravo have been able to characterise $\Phi_t(t')$ rigorously at large t for several long-range memory kernels and a wide class of resetting protocols [34]. In the case of a uniform memory kernel ($\lambda = 0$) and when the time intervals between resetting events are exponentially distributed (the resetting rate r is constant), their results stipulate that the rescaled variable

$$\xi = \frac{t' - \frac{1}{r}\ln(rt)}{\frac{1}{r}\sqrt{2\ln(rt)}}\tag{60}$$

becomes Gaussian distributed with zero mean and unit variance as $t\to\infty$. The general proof is carried out by applying the strong law of large numbers and central limits theorems on sums of independent and non-identically distributed random variables [34]. Hence $\Phi_t(t')$ is always time dependent, peaked around $t'^* = \frac{1}{r}\ln(rt)$ and with a much smaller standard deviation $\frac{1}{r}\sqrt{2\ln(rt)}$. These features contrast with the function $\varphi_t(t')$ in Eq. (57), which tends toward the stationary exponential distribution $\varphi_\infty(t') = re^{-rt'}$ and whose mean and standard deviation are both equal to 1/r. To leading order for large t, the limiting form in Eq. (60) suggests that $\Phi_t(t')$ can be approximated by a delta function centered at the mean, i.e., $\Phi_t(t') \approx \delta(t'-t'^*)$ where $t'^* = \frac{1}{r}\ln(rt)$. Substituting the limit form of $\Phi_t(t')$ into Eq. (59), one recovers the distribution $P_r(\vec{x},t)$ at large t as a product of Gaussians with a variance growing as $2Dt'^* = \frac{2D}{r}\ln(rt)$, as shown by Eq. (35) in Section III B.

The decay of correlations between the components of $\vec{x}(t)$ at late times for $\lambda = 0$ is therefore a consequence of the growing characteristic time-scale t'^* associated with the paths \mathcal{P} . If $\lambda > 0$, in contrast, as discussed above, the joint distribution converges to a NESS and correlations persist as $t \to \infty$. The existence of a NESS implies that $\Phi_t(t')$ tends to a non-trivial stationary distribution $\Phi_{\infty}(t')$ in Eq. (59) as $t \to \infty$. As the particle mostly resets to positions visited early and belonging to the first diffusive paths $\{1, 2, 3, \ldots\}$, the paths \mathcal{P} remain short even after a very large number of resetting events. This situation is similar to resetting to the origin and the results of Mailler and Uribe Bravo do not apply to these cases, as they have considered memory kernels $K_t(\tau)$ which did not decay rapidly with τ

Eq. (59) further allows us to establish a simple general relation between the quantities P_r and Φ_t for Brownian motion, valid for any time t. In fact, for the preferential relocation model ($\lambda=0$), the relation between these two quantities also provides us with an alternative derivation of the result (60) of [34], namely that the centred and scaled variable ξ has a normal distribution of zero mean and unit variance. Let us proceed as follows. We first take the Fourier transform of Eq. (59) that gives

$$\tilde{P}_r(\vec{k}, t) = \int_0^\infty dt' \, \Phi_t(t') \, \prod_{i=1}^N \tilde{p}_0(k_i, t') \,, \tag{61}$$

where $\tilde{p}_0(k_i,t') = e^{-D k_i^2 t'}$ is simply the Fourier transform of the propagator of a Brownian motion in one dimension at time t'. Using $k^2 = \sum_{i=1}^N k_i^2$ then gives

$$\tilde{P}_r(\vec{k}, t) = \int_0^\infty dt' \, \Phi_t(t') \, e^{-D \, k^2 \, t'} \,. \tag{62}$$

Thus if $\tilde{P}_r(\vec{k},t)$ is known, we can invert this relation to determine $\Phi_t(t')$ in principle. For the preferential relocation model $(\lambda = 0)$, we know $\tilde{P}_r(\vec{k},t)$ exactly from Eq. (29). Substituting this result on the left-hand-side of (62), and replacing $D k^2$ by a new variable s for convenience, we get

$$\hat{\Phi}_t(s) = \int_0^\infty dt' \, \Phi_t(t') \, e^{-s \, t'} = M\left(\frac{s}{r+s}, 1, -(r+s)t\right) \,, \tag{63}$$

where $\hat{\Phi}_t$ is the Laplace transform of Φ_t . In the case $\lambda > 0$, an explicit but long expression can similarly be obtained from Eq. (47). Hence, for simplicity, let us focus on the $\lambda = 0$ case only. The Laplace transform in Eq. (63) can be

formally inverted to give

$$\Phi_t(t') = \int_{\Gamma} \frac{ds}{2\pi i} e^{st'} M\left(\frac{s}{r+s}, 1, -(r+s)t\right), \qquad (64)$$

where Γ denotes a vertical Bromwich contour in the complex s-plane whose real part lies to the right of all singularities of the integrand. An explicit inversion using (64), valid for all t, seems difficult. However, one can make progress for large t, where we can replace the function M by its asymptotic expansion, corresponding to the limit $u \to -\infty$ in Eq. (32). This gives, as $t \to \infty$ and fixed s,

$$M\left(\frac{s}{r+s}, 1, -(r+s)t\right) \approx \frac{1}{\Gamma\left(\frac{r}{r+s}\right)} e^{-\frac{s}{r+s}\ln[(r+s)t]}.$$
 (65)

Next, we want to investigate the behaviour of $\Phi_t(t')$ when both t' and t are large. For large t', the dominant contribution to the integral in Eq. (64) comes from the vicinity of small s, as we can shift the contour Γ close to s = 0. Hence we can now expand the integrand in Eq. (64) in small s. Substituting

$$\frac{s}{r+s} \ln[(r+s)t] \approx \frac{s}{r} \ln(rt) - \frac{s^2}{r^2} [\ln(rt) - 1] + O(s^3),$$
 (66)

in Eq. (65), we obtain from Eq. (64), when t and t' are both large,

$$\Phi_t(t') \approx \int_{\Gamma} \frac{ds}{2\pi i} e^{s[t' - \frac{1}{r} \ln(rt)] + \frac{s^2}{r^2} \ln(rt) + \dots},$$
(67)

where \dots denote higher order terms in s. Rescaling

$$s = \frac{r}{\sqrt{2\ln(rt)}}\,\tilde{s}\,,\tag{68}$$

and identifying the variable ξ in Eq. (60), we can re-write the integral in Eq. (67) as

$$\Phi_t(t') \approx \frac{r}{\sqrt{2\ln(rt)}} \int_{\Gamma} \frac{d\tilde{s}}{2\pi i} e^{\tilde{s}\,\xi + \frac{1}{2}\,\tilde{s}^2} \,. \tag{69}$$

Note that under the rescaling (68), all higher order terms in small s, beyond the quadratic one inside the exponential in Eq. (67), get rescaled by positive powers of $1/\sqrt{\ln(rt)}$ and hence disappear for large t. Finally, the integral in Eq. (69) is simple to perform exactly as it is just a Gaussian integral. This brings us to the final result that in the limit t and t' both large, but with the scaling combination ξ in Eq. (60) held fixed, the function $\Phi_t(t')$ approaches the scaling form

$$\Phi_t(t') \approx \frac{r}{\sqrt{2\ln(rt)}} f_0\left(\frac{t' - \frac{1}{r}\ln(rt)}{\frac{1}{r}\sqrt{2\ln(rt)}}\right), \quad \text{where} \quad f_0(\xi) = \frac{1}{\sqrt{2\pi}} e^{-\xi^2/2}.$$
(70)

This completes the derivation of the result in the preferential relocation model ($\lambda = 0$) that states that the centred and scaled variable ξ approaches a normal distribution with zero mean and unit variance at long times.

VI. CONCLUSIONS

We have studied the time evolution of the correlations between N independent one-dimensional diffusive processes starting from the origin and subject to simultaneous resetting, in cases where resetting occurs to positions visited in the past. This problem is equivalent to the study of the mutual correlations between the components of the position of a single N dimensional walker subject to resetting to positions visited in the past. One may consider, for instance, the (x_1, x_2) -coordinates of a random walker on the plane that revisits familiar places in its environment. We have chosen a memory kernel that interpolates, as a parameter λ is varied, between resetting to the starting position only (a memory-less process) and the preferential relocation model, which is strongly non-Markov. Our study provides an exact calculation of the full time-dependent emergence of the correlations in a non-Markov resetting model with memory, thus extending previous studies [21, 22, 26, 27] on the memory-less case.

For short-ranged memory kernels (large λ , similar to resetting to the origin) the correlation coefficient $a_{\lambda}(t)$ defined in Eq. (3) monotonically increases from 0 with time. Conversely, when memory is sufficiently long-range, correlations exhibit a non-monotonic behaviour with time and reach a maximum at a certain re-scaled time z^* . These two regimes are separated by a critical value λ_c of the parameter λ , where z^* diverges. For any non-zero λ , $a_{\lambda}(t)$ tends to a finite asymptotic value at large t. This persistent correlation depends only on λ and the resetting rate r through Eqs. (53)-(54). Therefore simultaneous resetting represents a robust mechanism by which strong correlations are built and maintained dynamically. The correlation is the largest in the case of resetting to the origin and $a_{\infty}(t \to \infty) = 1/5$ in that case, in agreement with previous results [21, 22].

The preferential relocation model (case $\lambda = 0$) is peculiar because the joint PDF of $(x_1(t), x_2(t))$ does not tend to a NESS and keeps depending on time at large times. We find that $a_0(t)$ is non-monotonous as well, but tends to 0 as $t \to \infty$. Hence the processes are uncorrelated at both short and large times. However, the decay of the correlations at late times is extremely slow, as $a_0(t) \simeq 1/\ln(rt)$.

We have finally shown that multi-dimensional processes subject to resetting (with or without memory) generally obey a conditionally i.i.d. structure at all times. This means that the joint distribution of the components of $\vec{x}(t)$ can be written under the form in Eq. (59). For instance, in the standard renewal approach of resetting to the origin, conditioning on the time t' elapsed since the latest reset, the positions $x_1(t)$ and $x_2(t)$ are independent. When memory is present, the renewal approach no longer holds $per\ se$ but the c.i.i.d. structure remains. In this case, the time t' is also the duration of a Brownian path that goes from the origin to the current position without any discontinuities, but it is formed by several pieces of previous Brownian paths, not just the latest one. Thus, the c.i.i.d structure of the joint distribution is not apparently manifest but remains hidden in this model, as in the case of another recently studied model of independent particles in a switching harmonic trap [23]. The challenge is to find the hidden c.i.i.d. structure explicitly because such a structure then guarantees exact computation of several physical observables in a relatively straightforward manner [23]. It would be interesting to seek other non-Markov systems with a c.i.i.d. structure.

Acknowledgements: DB acknowledges support from CONACYT (Mexico) Grant CF2019/10872 and from the University of Paris-Saclay, France (scientific missionary). SNM acknowledges support from ANR Grant No. ANR-23-CE30-0020-01 EDIPS. The authors thank the Isaac Newton Institute (Cambridge, UK) for hospitality during a stay where this work was initiated.

Appendix A: Large t asymptotics of $a_{\lambda=0}(t)$ in Eq. (11)

To compute $a_0(t)$ from the general exact expression in Eq. (11), we first need to consider the quadratic coefficient given by Eq. (41) and use the definition of $E_1(z) = \int_z^\infty \frac{dx}{x} e^{-x}$. One gets for large z = rt,

$$\frac{c_2^2(z)}{(D/r)^2} = \left[\ln z + \gamma_E + \frac{e^{-z}}{z} + \ldots\right]^2 = \ln^2 z + 2\gamma_E \ln z + \gamma_E^2 + O\left((\ln z) e^{-z}\right). \tag{A1}$$

Regarding the term $c_4(z)$ given by Eq. (42), it can be expanded at large z as

$$\frac{c_4(z)}{(D/r)^2} = \ln z + \gamma_E - 1 + \frac{1}{2} {}_{1}F_1^{(2,0,0)}(0,1,-z) + O\left(e^{-z}\right). \tag{A2}$$

So, the question is how the term ${}_{1}F_{1}^{(2,0,0)}(0,1,-z)$ behaves for large z. Unfortunately, Mathematica is unable to extract the asymptotic large t behavior of this term. So, we need to use the following trick. We note that by definition

$$_{1}F_{1}^{(2,0,0)}(0,1,-z) = \partial_{b}^{2}M(b,1,-z)\Big|_{b=0}$$
, (A3)

where M(b, c, u) is defined in Eq. (30). To evaluate (A3) for $z \gg 1$, we first use the asymptotic behaviour of M(b, c, u) for large negative u as given in Eq. (32). This gives for large t

$$M(b, 1, -z) = \frac{1}{\Gamma(1-b)} z^{-b} + O(z^{-b-1}).$$
(A4)

We now expand the rhs of (A4) for small b (but fixed large z) and from the coefficient of b^2 , we can read off the second derivative at b = 0 in Eq. (A3). This gives,

$$_{1}F_{1}^{(2,0,0)}(0,1,-z) = \ln^{2}z + 2\gamma_{E}\ln z + \gamma_{E}^{2} - \frac{\pi^{2}}{6} + \text{h.o.t}$$
 (A5)

where the higher order terms (h.o.t) decreases with large z. Consequently, we find that Eq. (A2) behaves as

$$\frac{c_4(z)}{(D/r)^2} = \frac{1}{2}\ln^2 z + (1+\gamma_E)\ln z + \frac{1}{2}\gamma_E^2 + \gamma_E - 1 - \frac{\pi^2}{12} + \text{h.o.t}$$
(A6)

where h.o.t again decreases for large z. Substituting (A6) and (A1) in Eq. (11) we get the final asymptotic tail of $a_0(t)$,

$$a_0(t) = \frac{1}{\ln z} - \frac{4 + \gamma_E + \frac{\pi^2}{12}}{\ln^2 z} + \dots$$
 (A7)

- [1] M. R. Evans and S. N. Majumdar, Diffusion with stochastic resetting, Phys. Rev. Lett. 106, 160601 (2011).
- A. Pal, Diffusion in a potential landscape with stochastic resetting, Phys. Rev. E 91, 012113 (2015).
- [3] S, N. Majumdar, S. Sabhapandit, and Grégory Schehr, Dynamical transition in the temporal relaxation of stochastic processes under resetting, Phys. Rev. E 91, 052131 (2015).
- [4] M. R. Evans and S. N. Majumdar, Diffusion with optimal resetting, J. Phys. A: Math. Theor. 44 435001 (2011).
- [5] A. Nagar and S. Gupta, Diffusion with stochastic resetting at power-law times, Phys. Rev. E 93, 060102 (2016).
- [6] S. Eule and J. J. Metzger, Non-equilibrium steady states of stochastic processes with intermittent resetting, New J. Phys. 18, 033006 (2016).
- [7] A. Pal, L. Kúsmierz, and S. Reuveni, Time-dependent density of diffusion with stochastic resetting is invariant to return speed, Phys. Rev. E 100, 040101 (2019).
- [8] A. S. Bodrova and I. M. Sokolov, Resetting processes with noninstantaneous return, Physical Review E 101, 052130 (2020).
- [9] M. R. Evans, S. N. Majumdar, and G. Schehr, Stochastic resetting and applications, J. Phys. A 53, 193001 (2020).
- [10] O. Tal-Friedman, A. Pal, A. Sekhon, S. Reuveni, and Y. Roichman, Experimental Realization of Diffusion with Stochastic Resetting, J. Phys. Chem. Lett. 11, 7350 (2020).
- [11] B. Besga, A. Bovon, A. Petrosyan, S. N. Majumdar, and S. Ciliberto, Optimal mean first-passage time for a Brownian searcher subjected to resetting: experimental and theoretical results, Phys. Rev. Research 2, 032029(R) (2020).
- [12] F. Faisant, B. Besga, A. Petrosyan, S. Ciliberto, and S. N. Majumdar, Optimal mean first-passage time of a Brownian searcher with resetting in one and two dimensions: experiments, theory and numerical tests, J. Stat. Mech. 113203 (2021).
- [13] M. R. Evans and S. N. Majumdar, Diffusion with resetting in arbitrary spatial dimension, J. Phys. A 47, 285001 (2014).
- [14] S. Gupta, S. N. Majumdar, and G. Schehr, Fluctuating interfaces subject to stochastic resetting, Phys. Rev. Lett., 112, 220601 (2014).
- [15] R. Falcao and M. R. Evans, Interacting Brownian motion with resetting, J. Stat. Mech. 023204 (2017).
- [16] U. Basu, A. Kundu, and A. Pal, Symmetric exclusion process under stochastic resetting, Phys. Rev. E 100, 032136 (2019).
- [17] M. Magoni, S. N. Majumdar, and G. Schehr, Ising model with stochastic resetting, Phys. Rev. Research, 2, 033182 (R) (2020).
- [18] R. Majumder, R. Chattopadhyay, and S. Gupta, Kuramoto model subject to subsystem resetting: How resetting a part of the system may synchronize the whole of it, Phys. Rev. E 109, 064137 (2024).
- [19] A. Biswas, S. N. Majumdar, and A. Pal, Target search optimization by threshold resetting, arXiv: 2504.13501.
- [20] A. Nagar and S. Gupta, Stochastic resetting in interacting particle systems: a review J. Phys. A: Math. Theor. **56**, 283001 (2023).
- [21] M. Biroli, H. Larralde, S. N. Majumdar, and G. Schehr, Extreme statistics and spacing distribution in a Brownian gas correlated by resetting, Phys. Rev. Lett., 130, 207101 (2023).
- [22] M. Biroli, H. Larralde, S. N. Majumdar, and G. Schehr, Exact extreme, order and sum statistics in a class of strongly correlated system, Phys. Rev. E 109, 014101 (2024).
- [23] M. Biroli, M. Kulkarni, S. N. Majumdar, and G. Schehr, Dynamically emergent correlations between particles in a switching harmonic trap, Phys. Rev. E 109, L032106 (2024).
- [24] S. Sabhapandit and S. N. Majumdar, Noninteracting particles in a harmonic trap with a stochastically driven center, J. Phys. A: Math. Theor. 57, 335003 (2024).
- [25] N. Mesquita, S. N. Majumdar, and S. Sabhapandit, Dynamically emergent correlations in a Brownian gas with diffusing diffusivity, arXiv: 2506.20859.
- [26] G. de Mauro, M. Biroli, S. N. Majumdar, and G. Schehr, Dynamically emergent correlations in Brownian particles subject to simultaneous non-Poissonian resetting protocols, arXiv: 2509.06658.
- [27] M. Biroli, S. Ciliberto, M. Kulkarni, S. N. Majumdar, A. Petrosyan, and G. Schehr, Experimental evidence for strong emergent correlations between particles in a switching trap, arXiv: 2508.07199.
- [28] M. Magoni, F. Carrolo, G. Perfetto, and I. Lesanovsky, Emergent quantum correlations and collective behavior in noninteracting quantum systems subject to stochastic resetting, Phys. Rev. A 106, 052210 (2022).
- [29] D Soldner, I Lesanovsky, and G Perfetto, Nonanaliticities and ergodicity breaking in noninteracting many-body dynamics via stochastic resetting and global measurements, arXiv: 2510.11450

- [30] M. Kulkarni, S. N. Majumdar, and S. Sabhapandit, Dynamically emergent correlations in bosons via quantum resetting, J. Phys. A 58, 105003 (2025).
- [31] N. Mesquita, M. Kulkarni, S. N. Majumdar, and S. Sabhapandit, Dynamically generated correlations in a trapped bosonic gas via frequency quenches, arXiv: 2509.00487.
- [32] D. Boyer and C. Solis-Salas, Random walks with preferential relocations to places visited in the past and their application to biology, Phys. Rev. Lett. 112, 240601 (2014).
- [33] D. Boyer, M. R. Evans, and S. N. Majumdar, Long time scaling behaviour for diffusion with resetting and memory, J. Stat. Mech. 023208 (2017).
- [34] C. Mailler and G. Uribe Bravo, Random walks with preferential relocations and fading memory: a study through random recursive trees, J. Stat. Mech. 093206 (2019).
- [35] A. O. Gautestad and I. Mysterud, Intrinsic scaling complexity in animal dispersion and abundance, Am. Nat. 165, 44 (2005).
- [36] C. Song, T. Koren, P. Wang, and A.-L. Barabási, Modelling the scaling properties of human mobility, Nature Physics 6, 818 (2010).
- [37] W. F. Fagan, M. A. Lewis, M. Auger-Méthé, T. Avgar, S. Benhamou, G. Breed, L. LaDage, U. E. Schlägel, W.-w. Tang, Y. P. Papastamatiou, et al., Spatial memory and animal movement, Ecol. Lett. 16, 1316 (2013).
- [38] J. Merkle, D. Fortin, and J. M. Morales, A memory-based foraging tactic reveals an adaptive mechanism for restricted space use, Ecol. Lett. 17, 924 (2014).
- [39] A. Falcón-Cortés, D. Boyer, E. Merrill, J. L. Frair, and J. M. Morales, Hierarchical, memory-based movement models for translocated Elk (Cervus canadensis), Front. Ecol. Evol 9, 702925 (2021).
- [40] N. Ranc, P. R. Moorcroft, F. Ossi, and F. Cagnacci, Experimental evidence of memory-based foraging decisions in a large wild mammal, Proc. Natl. Acad. Sci. USA 118, e2014856118 (2021).
- [41] N. Ranc, F. Cagnacci, and P. R. Moorcroft, Memory drives the formation of animal home ranges: evidence from a reintroduction, Ecol. Lett. 25, 716 (2022).
- [42] M. Abramowitz and I. A. Stegun (Eds.), Handbook of Mathematical Functions with Formulas, Graphs, and Mathematical Tables (Dover, New York, 1965).
- [43] G. I. Barenblatt, Scaling, Self-similarity, and Intermediate Asymptotics (Cambridge, Cambridge, UK, 1996).